JOURNAL OF MATERIALS SCIENCE **40** (2005) 6175–6180

Study on mechanism of iron reduction in magnesium alloy melt

GUO HUA WU, HONG TAO GAO*, WEN JIANG DING, YAN PING ZHU
State Key Laboratory of Metal Matrix Composites, School of Materials Science and Engineering, Shanghai Jiao Tong University, Shanghai, 200030, People's Republic of China
E-mail: hunter@sjtu.edu.cn

Published online: 8 September 2005

This article studies the mechanism of iron reduction in magnesium alloy melt by investigating the iron concentrations in different parts in the melt with different holding time. The iron concentrations at the top, the center and the bottom of the melt are measured with the holding time of 300, 1800 and 7200 s. The elements in the sludge settling down in the crucible are also determined by ICP. With the increasing holding time, the iron content in the upper part of the melt decreases and that in the lower part of the melt increases. And the iron content in the sludge increases rapidly. The iron concentrations in the melt and the sludge change little with longer holding time than 1800 s. Among the three iron reduction agents B_2O_3, $MnCl_2$ and TiO_2, B_2O_3 has the highest iron reduction efficiency (IRE). IRE of B_2O_3 is as two times and five times as IRE of $MnCl_2$ and IRE of TiO_2 respectively. Formation of FeB and settling of it into melting sludge are believed to be the primary mechanism of iron reduction by B_2O_3 processing. The mechanism of iron reduction in magnesium melt by $MnCl_2$ or TiO_2 processing is studied by thermodynamic analysis. Formation of substance containing MnFeAl or TiFe with high density and high melting point and settling of them into melting sludge are suggested to be the mechanism of iron reduction by $MnCl_2$ or TiO_2 processing.

1. Introduction

The magnesium alloy, as the lightest structural metal, has been widely used in automobile, electronics and aerospace industries due to its desirable combination of properties, including low density, high specific strength and specific stiffness, superb damping and electromagnetic shielding capacities, good machinability, and good castability [1, 2]. The demand for magnesium alloys has been increasing significantly since 1990 s [3–6].

The inherent quality of magnesium alloys, as we know, to a critical level is the prerequisite for that many processing techniques take effects to a satisfactory extent. Therefore, we make great efforts to improve the inherent quality of magnesium alloy ingots. In magnesium alloys, iron must be controlled to an extremely low level because even a small amount of it can remarkably impair the corrosion resistance [7–9]. In addition, iron is reported to suppress grain-refining effects of super-heating treatment [10, 11].

In a previous paper [12], the author studied the iron reduction in AZ91 melts by B_2O_3. However, the mechanism of iron reduction was not further discussed. In this article the author studied the mechanism of iron reduction in magnesium melt by investigating the iron concentrations in different parts in the melt with different holding time. The experimental iron reduction agents are B_2O_3 [12], $MnCl_2$ and TiO_2 [13]. The author also compared the effects of B_2O_3, $MnCl_2$ and TiO_2 on iron reduction in magnesium melt.

2. Experimentals

2.1. Materials

Industrial AZ91 alloy scraps with initial iron content of 0.062 wt% were adopted in this work. Chemically pure B_2O_3, $MnCl_2$ or TiO_2 was mixed with a purification flux named JDMR flux (mainly chloride) [14], respectively, and then added into the melt for iron reduction. The JDMR flux was developed by Shanghai Jiao Tong University.

2.2. Experimental procedures

The scraps were melted in a graphite crucible under protection of a shield gas consisting of SF_6 (1 vol%) and CO_2 (bal.). The mixtures of B_2O_3, $MnCl_2$ or TiO_2 and the JDMR flux in the form of powder were added into the melt at the temperature of 735–740°C respectively. The addition of the mixture was 4 wt% by the melt

*Author to whom all correspondence should be addressed.
0022-2461
DOI: 10.1007/s10853-005-3161-7

weight. And the iron reduction agent is 20 wt% by the mixture. After being stirred for fifteen minutes, the melt was held for 300, 1800 and 7200 s and samples at the top, the center and the bottom of the melt were got for chemical analysis. The sludge that deposited at the crucible bottom was also collected for chemical analysis.

The chemical compositions of the melts and the sludge were studied with an inductively coupled plasma spectrum machine (ICP, IRIS Advantage 1000) produced by the Thermo Jarrell Ash Company. Phases were analyzed using a scanning electron microscope (SEM, PHILIP SEM515) with an energy dispersive spectroscope (EDS). The sludge was studied by means of an X-ray diffractometer (XRD, Rigaku Dmax-rC).

3. Results

3.1. Iron distribution in the melts and the sludge

Fig. 1a–c show the distribution of iron and boron in the melts and the sludge with the holding time of 300, 1800 and 7200 s respectively. It can be seen that the iron content and the boron content increase from the top to the bottom in the melts, but the increasing extent is not significant with the holding time of 300 s. The sludge has the highest iron content and boron content. With the holding time of 1800 and 7200 s, the iron distribution and the boron distribution appear similar with that for 300 s. However, the iron and the boron in the sludge are far more than those in the melts. In addition, the iron distribution shows little difference with the holding time of 1800 and 7200 s. Therefore, it is presumed that iron atoms have almost settled down in the sludge within 1800 s. And 1800 s is believed to be the proper holding time for B_2O_3 processing.

Fig. 2a–c show the iron distribution and the manganese distribution in the $MnCl_2$ processed melt and the sludge. The experimental results are similar with those of the B_2O_3 processing. A little difference lies in the fact that the $MnCl_2$ processed melt has high manganese content which is due to manganese in the original AZ91 ingot. However, the highest manganese content in the sludge shows us that manganese atoms react with other atoms and form some high density substance settling down in the crucible.

Fig. 3a–c show the iron distribution and the titanium distribution in the TiO_2 processed melt and the sludge. The experimental results are similar with those of the B_2O_3 processed melt. We can presume that titanium atoms react with other atoms, probably iron, and form some high density substance settling down in the melts.

3.2. Iron reduction efficiency

The changes of the iron concentration in different parts in the melts with the increasing holding time were shown in Fig. 4a–c. It can be seen that iron decreases with the increasing holding time for the top, the center and the bottom melts in the crucible. And a sharp drop appears with the holding time of 300 and 1800 s. The iron content changes little with the holding time increasing from 1800 to 7200 s. At the same part in the melt, iron decreases more quickly in the B_2O_3 processed melt than that in the $MnCl_2$ processed melt or the TiO_2 processed melt.

TABLE I Changes of iron concentration in different parts of the melt with the holding time of 300 s

	ΔC_{Fe} (wt%)		
Samples	Top	Center	Bottom
B_2O_3 processed melt	0.032	0.026	0.016
$MnCl_2$ processed melt	0.020	0.011	0.005
TiO_2 processed melt	0.011	0.005	0.003

Table I shows the changes of iron concentration (represented by ΔC_{Fe}) in different parts in the melts with the holding time of 300 s. We define ΔC_{Fe} in the center part of the melts as iron reduction efficiency (represented by IRE). IRE is 0.026, 0.011 and 0.005 for B_2O_3, $MnCl_2$ and TiO_2 processing respectively. Therefore, B_2O_3 is believed as an effective iron reduction agent for magnesium.

4. Discussion

Generally, it is difficult to study the reactions that occur in a chemically complicated alloy melt by experiments. Therefore, we tried to analyze the reactions via thermodynamic calculations in B_2O_3 processed, $MnCl_2$ processed and TiO_2 processed magnesium melts, respectively. The related thermodynamic data come from two handbooks [15, 16].

(1) B_2O_3: In the B_2O_3 processed melt, the following reactions may take place concerning B_2O_3, Mg and Fe.

$$B_2O_3\,(s) + 3Mg\,(l) = 3MgO\,(s) + 2B\,(s) \quad (1)$$
$$\Delta G_1^0 = -1828710 + 106.16T$$

$$B\,(s) + Fe\,(l) = FeB\,(s) \quad (2)$$
$$\Delta G_2^0 = -93300 + 18.07T$$

$$B\,(s) + 2Fe\,(l) = Fe_2B\,(s) \quad (3)$$
$$\Delta G_3^0 = -128940 + 35.26T$$

$$B_2O_3\,(s) + 3Mg\,(l) + 2Fe\,(l) = 3MgO\,(s) + 2FeB\,(s) \quad (4)$$

$$B_2O_3\,(s) + 3Mg\,(l) + 4Fe\,(l) = 3MgO\,(s) + 2Fe2B\,(s) \quad (5)$$

Here s, l and g represent solid, liquid and gas respectively, ΔG_1^0, ΔG_2^0 and ΔG_2^0 are the changes of Gibbs free energy of reactions (1), (2) and (3) at standard state (1 atmosphere and 298 K) respectively, T is the reaction temperature, and R is thermodynamic constant.

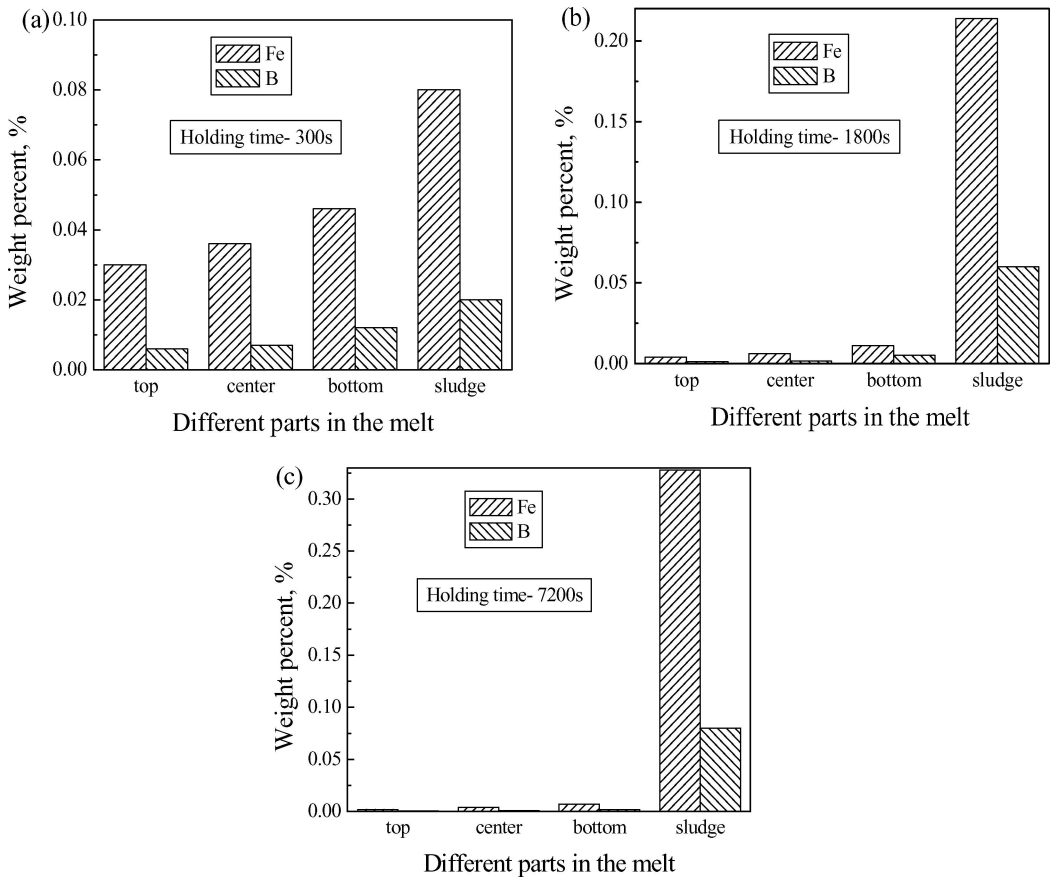

Figure 1 Iron and boron distributions in the B_2O_3 processed melt and the sludge with different holding time (a) 300 s, (b) 1800 s, and (c) 7200 s.

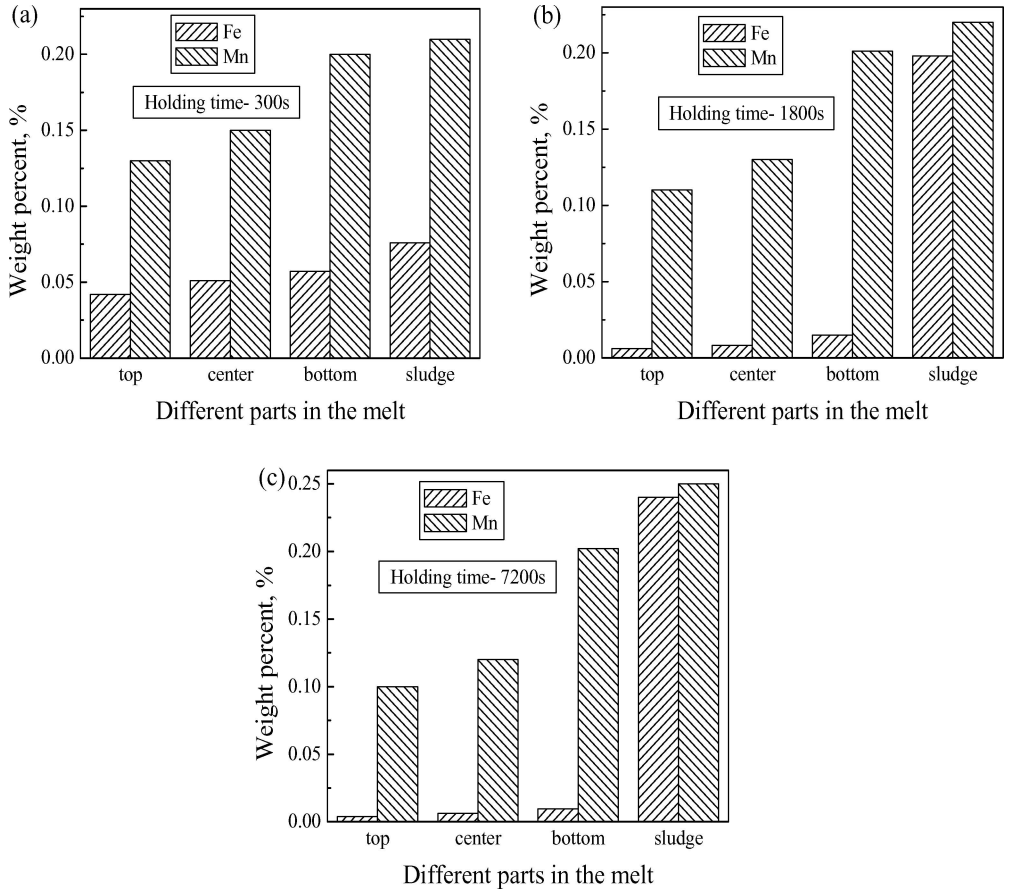

Figure 2 Iron and manganese distributions in the $MnCl_2$ processed melt and the sludge with different holding time (a) 300 s, (b) 1800 s, and (c) 7200 s.

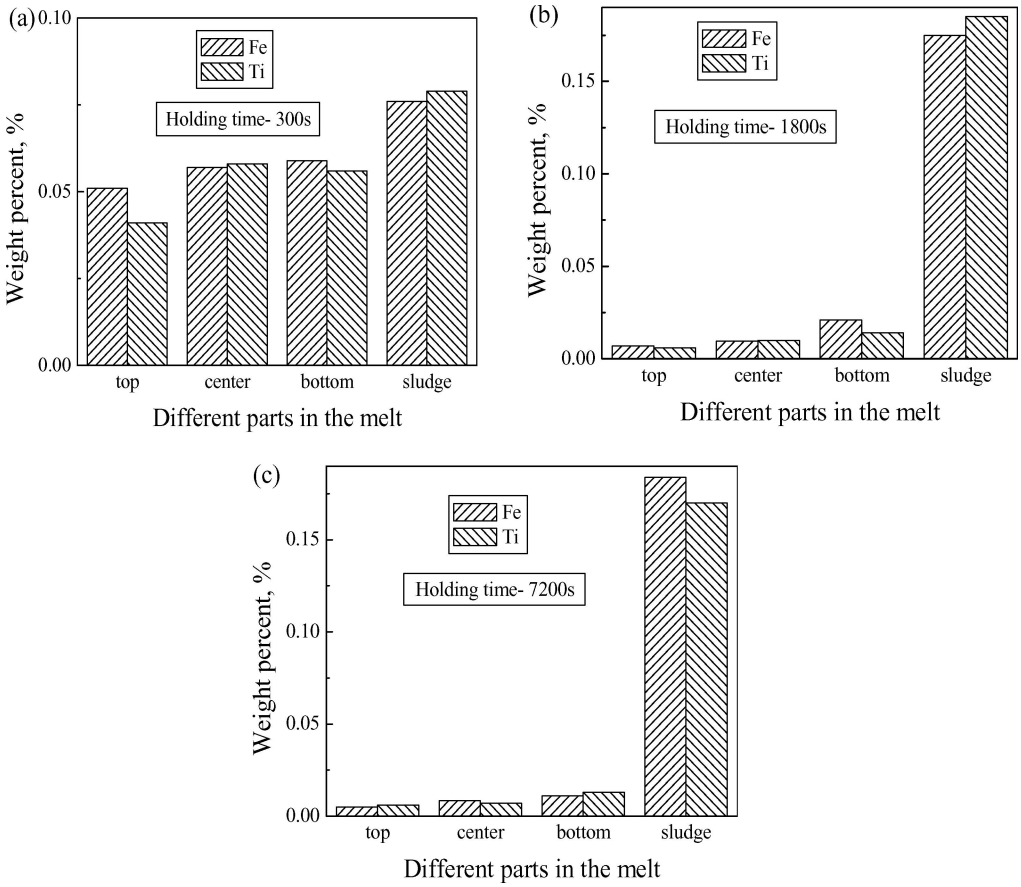

Figure 3 Iron and titanium distributions in the TiO_2 processed melt and the sludge, with different holding time (a) 300 s, (b) 1800 s, and (c) 7200 s.

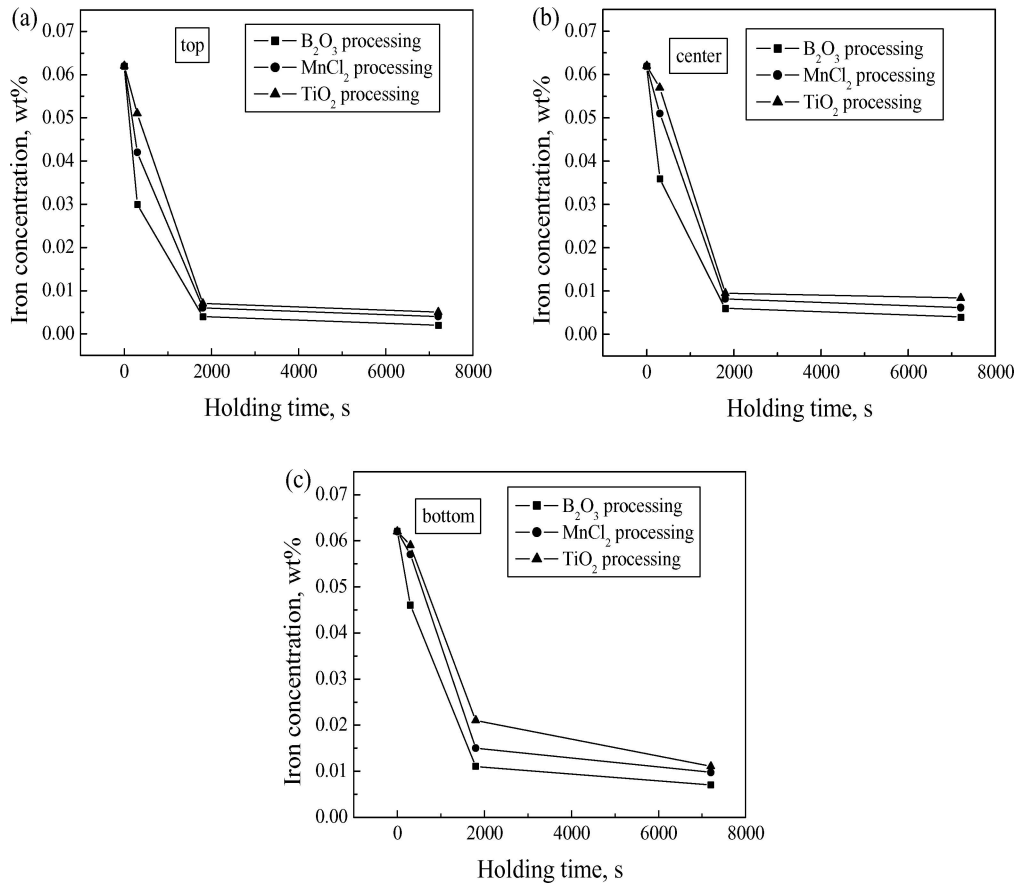

Figure 4 Changes of iron content with increasing holding time at different parts of the melts (a) top, (b) center, and (c) bottom.

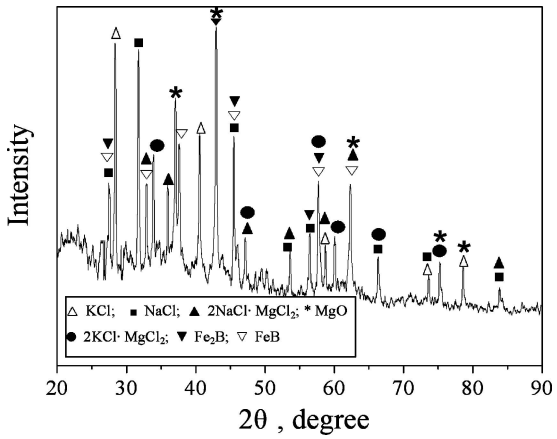

Figure 5 X-ray diffraction spectrum of the melting sludge.

The change of standard Gibbs free energy of the reaction (4) is calculated:

$$\Delta G_4^0 = \Delta G_1^0 + \Delta G_2^0 \times 2 = -2015310 + 142.3T$$
$$= -1972905\ (\mathrm{J/mol}) < 0$$
$$\Delta G_5^0 = \Delta G_1^0 + \Delta G_3^0 \times 2 = -2086590 + 176.68T$$
$$= -2033939\ (\mathrm{J/mol}) < 0$$

ΔG_4^0 and ΔG_5^0 are negative at the standard state, indicating that the reactions (4) and (5) are spontaneous thermodynamically.

Taking T as 1008 K, ΔG_4^0 and ΔG_5^0 can be calculated:

$$\Delta G_4^0 = -2015310 + 142.3T$$
$$= -1871871.6\ (\mathrm{J/mol}) < 0$$
$$\Delta G_5^0 - 2086590 + 176.68T$$
$$= -1908496.6\ (\mathrm{J/mol}) < 0$$

which indicate that FeB and Fe_2B can occur in the B_2O_3 processed melt at 1008 K. According to the ratio of B (corresponding to B_2O_3) addition and Fe content in the melt, B is excess so that the reaction (2) play a major role in removing Fe. The reaction (3) can only take place in case of insufficient B based on optimal chemical equilibrium. In the real, not optimal condition, however, the reaction (3) may also take place in some extent in spite of very little formation of Fe_2B. In the XRD analysis pattern shown in Fig. 5 FeB (its melting point is 1650°C) [17] was detected in the sludge. And little Fe_2B may also exist, but it is not certain because its all peaks are overlapped.

(2) $MnCl_2$: The similar work as the B_2O_3 processing was carried out for the $MnCl_2$ processed melt as follows.

$$\mathrm{MnCl_2\,(s) + Mg\,(l) = MgCl_2\,(l) + Mn\,(l)} \qquad (6)$$

At 1008 K, the change of Gibbs free energy of the reaction (6) ΔG_6^0 is calculated:

$$\Delta G_6^0 = -29270 - 73.05T$$
$$= -102904.4\ (\mathrm{J/mol}) < 0$$

which indicates that manganese can be substituted by magnesium in the $MnCl_2$ processed melt. These manganese atoms react with iron atoms and form some intermetallic containing MnFeAl settling down in the crucible. The phase containing MnFeAl was observed in the lower part of the melt by SEM. Fig. 6a and b are morphology and EDS result of the phase respectively.

(3) TiO_2: The similar work as the B_2O_3 processing was carried out for the TiO_2 processed melt as follows.

$$\mathrm{TiO_2\,(s) + 2Mg\,(l) = Ti\,(s) + 2MgO\,(s)} \qquad (7)$$

At 1008 K, The change of Gibbs free energy of the reaction (7) ΔG_7^0 is calculated:

$$\Delta G_7^0 = -262660 + 47.52T$$
$$= -214759.8\ (\mathrm{J/mol}) < 0$$

which indicates that titanium can be obtained in the TiO_2 processed melt. And Ti was reported to react with Fe and settles down [18] in the crucible. Unfortunately we have not detected some compound containing Fe and Ti in the melt or sludge. And we will further work on it.

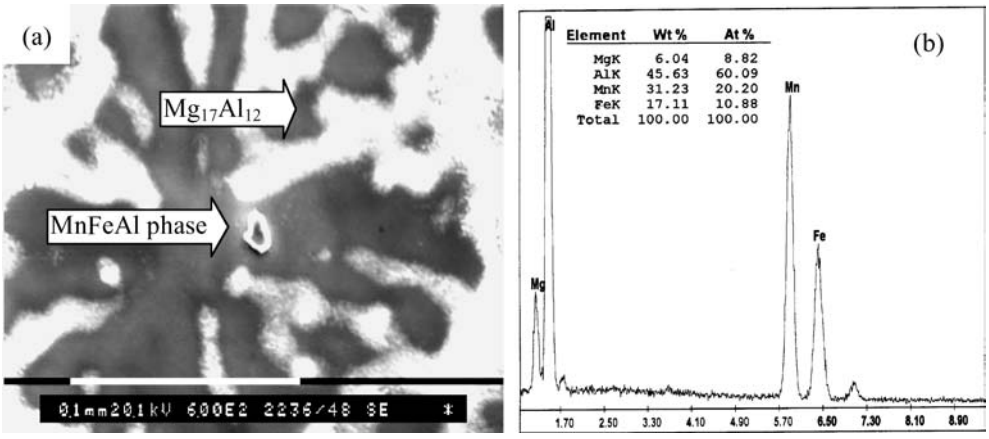

Figure 6 Morphology of the MnFeAl phase and its EDS result.

5. Conclusions

1. The iron concentration decreases significantly in the magnesium melt by B_2O_3, $MnCl_2$ or TiO_2 processing. The iron concentration in the upper part of the melt is smaller than that in the lower part of the melt. And the sludge has the highest iron content.

2. The iron concentration in the melt decreases sharply within the holding time of 1800 s. And the iron reduction efficiency of B_2O_3 is higher than that of $MnCl_2$ or TiO_2.

3. Thermodynamic analysis and XRD research show that formation of FeB is the main reason for iron reduction in the magnesium melt. The iron reduction in the $MnCl_2$ or TiO_2 processed melts is due to formation of the high density substance containing FeMnAl or FeTi settling down in the crucible.

Acknowledgement

The present study is funded by the National High Technology R&D Program of China and the National Natural Science Foundation of China.

References

1. J. E. GRAY and B. LUAN, *J. All. Comp.* **336** (2002) 88.
2. H. FURUYA, N. KOGISO, S. MATUNAGA and K. SENDA, *Mater. Sci. Forum* **350** (2000) 341.
3. R. BROWN, *Light Metal Age* **58**(9/10) (2000) 54.
4. R. P. PAWLEK and R. B. BROWN, *ibid.* **59**(8) (2001) 50.
5. S. KLEINER, O. BEFFORT, A. WAHLEN and P. J. UGGOWITZER, *J. Light Metals* **2** (2002) 277.
6. E. B. ROBERT, *Light Metal Age* **61**(1/2) (2003) 53.
7. T. HAITANI, Y. TAMURA, T. MOTEGI, N. KONO and H. TAMEHIRO, *Mater. Sci. Forum* **419/422** (2003) 697.
8. J. D. HANAWALT, *Trans. AIME* **147** (1942) 279.
9. M. INOUE, M. IWAI, K. MATUZAWA, S. KAMADO and Y. KOJIMA, *J. Japan Inst. Light Metals* **48**(6) (1998) 257.
10. Y. TAMURA, T. MOTEGI, N. KONO and E. SATO, *Mater. Sci. Forum* **350/351** (2000) 199.
11. T. HAITANI, Y. TAMURA, E. YANO, T. MOTEGI, N. KONO and E. SATO, *J. Japan Inst. Light Met.* **51** (2001) 403.
12. H. GAO, G. WU, W. DING, L. LIU, X. ZENG and Y. ZHU, *Mater. Sci. Engng* **A368** (2004) 311.
13. G. WU, C. ZHAI, X. ZENG, W. DING and Y. ZHU, *Acta Metall. Sinica* **39** (2003) 729.
14. G. WU, M. XIE, C. DI, X. ZENG, Y. ZHU and W. DING, *Trans. Nonferr. Met. Soc. China* **13** (2003) 1260.
15. Y. LINAG, Y. CHE and X. LIU, "Handbook of Inorganic Thermodynamic Data" (North-East University Press, Shenyang, 1993).
16. R. KUZMAN, "Handbook of Thermodynamic Tables and Charts" (Hemisphere Publishing Corporation, Washington, 1976).
17. E. T. TURKDOGAN, "Physical Chemistry of High Temperature Technology" (Academic Press, New York, 1980) p. 25.
18. R. XU, "Magnesium Metallurgy" (Metallurgy Industry Press, Beijing, 1993), p. 314.

Received 27 April 2004
and accepted 28 April 2005